Zootaxa 5380 (3): 247–264
https://www.mapress.com/zt/

Article

ISSN 1175-5326 (print edition)
ZOOTAXA
ISSN 1175-5334 (online edition)

https://doi.org/10.11646/zootaxa.5380.3.3
http://zoobank.org/urn:lsid:zoobank.org:pub:E9D5E0AF-9A3D-4C32-9C0A-6CCF5609D87E

Morphology of the larvae of *Rhantaticus congestus* (Klug, 1833) and phylogenetic comparison with other known Aciliini (Coleoptera: Dytiscidae: Dytiscinae)

YVES ALARIE[1*], MARIANO C. MICHAT[2], JOHANNES BERGSTEN[3] & JIŘÍ HÁJEK[4]
[1] *School of Natural Sciences, Laurentian University, Ramsey Lake Road, Sudbury, Ontario, Canada.*
yalarie@laurentian.ca; *https://orcid.org/0000-0002-8425-087X*
[2] *University of Buenos Aires, Faculty of Exact and Natural Sciences, Department of Biodiversity and Experimental and Applied Biology (IBBEA), Buenos Aires, Argentina.*
marianoide@gmail.com; *https://orcid.org/0000-0002-1962-7976*
[3] *Department of Zoology, Swedish Museum of Natural History, P.O. Box 50007, 10405 Stockholm, Sweden.*
johannes.bergsten@nrm.se; *https://orcid.org/0000-0002-6153-4431*
[4] *Department of Entomology, National Museum, Cirkusová 1740, CZ-193 00 Praha 9 – Horní Počernice, Czech Republic.*
jiri.hajek@nm.cz; *https://orcid.org/0000-0001-5779-1542*
** Corresponding author*

Abstract

We describe the second- and third instar larvae of the diving beetle *Rhantaticus congestus* (Klug, 1833), including detailed morphometric and chaetotaxic analyses of the cephalic capsule, head appendages, legs, terminal abdominal segment and urogomphi in order to discover useful characters for distinguishing *Rhantaticus* Sharp, 1882 larvae from those of other known Aciliini (Coleoptera: Dytiscidae: Dytiscinae). A parsimony analysis based on 94 larval characteristics of nine Aciliini species in five genera (*Acilius* Leach, 1817, *Graphoderus* Dejean, 1833, *Rhantaticus*, *Sandracottus* Sharp, 1882, *Thermonectus* Dejean, 1833) was conducted using the program TNT. *Rhantaticus* shares with all these genera several larval character states which support its inclusion in the Aciliini. Whereas *Rhantaticus* larva stands out from other known genera by several unique character states, our parsimony analysis did not recover any clear phylogenetic position of this genus within the Aciliini.

Key words: Coleoptera, Dytiscidae, Eretini, Aubehydrini, *Rhantaticus*, Madagascar, larvae, morphometry, chaetotaxy, phylogeny

Introduction

Rhantaticus congestus (Klug, 1833) is the only species of diving beetle in the genus *Rhantaticus* Sharp, 1882 (Coleoptera: Adephaga: Dytiscidae). With regard to its distribution *R. congestus* is one of the most widespread dytiscid species in the world, found throughout much of Africa, the Middle East, India, Southeast Asia, and the Philippines to Australia (Miller & Bergsten 2016; Nilsson & Hájek 2023). This genus belongs to the tribe Aciliini, subfamily Dytiscinae, along with *Acilius* Leach, 1817, *Aethionectes* Sharp, 1882, *Graphoderus* Dejean, 1833, *Sandracottus* Sharp 1882, *Thermonectus* Dejean, 1833, and *Tikoloshanes* Omer-Cooper, 1956 (Nilsson & Hájek 2023). Aciliini include medium to large-sized beetles (7.5–18.2 mm) generally found in ponds, marshes and other lentic habitats (Miller & Bergsten 2016). The monophyletic origin of this group and its relationship with the Dytiscinae tribes Eretini, Hydaticini, and Aubehydrini is no longer in doubt as demonstrated by numerous studies involving larval, adult and molecular characters (Miller 2001, 2003; Miller *et al*. 2007; Michat & Alarie 2009; Alarie *et al.* 2011, 2023b; Bukontaite *et al.* 2014; Michat *et al.* 2017; Miller & Bergsten 2023).

The recent discovery of the second and third instar larvae of *R. congestus* prompted this article. Except for a few superficial illustrations produced by Bertrand (1972), larvae of *Rhantaticus* remain unknown. Despite the fact that the first larval stage of *Rhantaticus* remains unknown, a detailed description of the second and third instar is all the more relevant as it opens the way to a phylogenetic comparison with the Aciliini genera whose larvae have been described (i.e., *Acilius*, *Graphoderus Thermonectus*, *Sandracottus*) according to the now generalized

Accepted by H. Fery: 10 Nov. 2023; published: 30 Nov. 2023

larval descriptive format of Dytiscidae, which incorporates detailed chaetotaxic (see Alarie & Michat 2023 for a comprehensive synthesis) and morphometric analyses (Alarie *et al.* 2011, 2023a, 2023b; Michat 2013; Michat & Torres 2005, 2016; Michat *et al*. 2017). In this respect, the comparison of the larva of *Rhantaticus* with those of the genus *Sandracottus* proves to be most interesting knowing that molecular data suggest a sister group relationship between these two genera (Bukontaite *et al.* 2014).

Material and methods

Habitus photographs of larvae in alcohol were taken using a Canon EOS 550D digital camera with an attached Canon MP-E65mm f/2.8 1–5× macro lens as numerous separate images at different focal planes and afterwards combined using Helicon Focus 6.3.0 software. Larvae were disarticulated and mounted on standard glass slides in Hoyer's medium. Microscopic examination at magnifications of 80–800× was done using an Olympus BX50 compound microscope equipped with Nomarsky differential interference optics. Figures were prepared through use of a drawing tube attached to the microscope. Drawings were scanned and digitally inked using an Intuos 4 professional pen tablet (Wacom Co., Ltd. Kazo, Saitama, Japan). The specimens included in this study are deposited in the National Museum, Prague, Czech Republic (J. Hájek), the Swedish Museum of Natural History, Stockholm, Sweden (J. Bergsten) and in the larval collection of Y. Alarie (School of Natural Sciences, Laurentian University, Canada).

The identity of the larvae is confirmed through two lines of evidence. First by co-sampling of larvae and adults at the same time and locality. Second by linking some larva with identified adults using DNA sequence data. One (NHRS-JLKB000000097) of the here studied instar II larvae (MAD09-47 at Kirindy RS) was sequenced for COI, COII, 16S, WNT, CAD and 28S and included in the analysis by Bukontaite *et al.* (2014) (see that study for methods and details of primers, gene fragments and GenBank accession codes). The larva unambiguously group with other sequenced adults of *R. congestus* confirming the identity.

Rhantaticus congestus larvae are described following the approach favored recently in the study of Aciliini larvae (Alarie *et al.* 2023a, 2023b). In the morphometric analysis, the following measurements were taken (with abbreviations shown in parentheses): head length (HL), total head length including the frontoclypeus, measured medially along the epicranial stem; maximum head width (HW); length of frontoclypeus (FRL), measured from apex of nasale to the joint of frontal and coronal sutures; occipital foramen width (OCW), maximum width measured along dorsal margin of occipital foramen; coronal line length (COL); length of mandible (MNL), measured from laterobasal angle to apex; width of mandible (MNW), maximum width measured at base; lengths of antenna (A), maxillary (MP) and labial (LP) palpi were obtained by adding the lengths of the individual segments, each segment is denoted by the corresponding letter(s) followed by a number (e.g., A1, first antennomere), A3' is used as an abbreviation for the apical lateroventral process of the third antennomere; length of maxillary palpifer (PPF); length of galea (GA); length of prementum median process (PMP), measured ventrally; length of leg (L), including the longest claw (CL), was obtained by adding the lengths of the individual segments; each leg is denoted by the letter L followed by a number (e.g., L1, prothoracic leg); the length of trochanter includes only the proximal portion, the length of distal portion is included in the femoral length; dorsal length of terminal abdominal segment (LAS), measured along midline from anterior to posterior margin; length of urogomphus (U) is its total length from base to apex. These measurements were used to calculate several ratios that characterize body shape.

Although represented by instars II and III only, primary setae and pores (present in first instar larva) of *Rhantaticus* were tentatively inferred by comparison with the Aciliini ground plan (Alarie *et al*. 2011, 2023b; Michat *et al.* 2017) wherever possible. In these cases, homologies were recognized using the criterion of similarity of position (Wiley 1981). As far as possible, the primary sensilla have been identified and represented on different structures of the second instar larva. It is important to emphasize, however, that absence of some primary setae and pores in figures should not be interpreted as a characteristic of the *Rhantaticus* larva rather as an inability on our part to identify safely either their presence or absence due often to the presence of secondary sensilla (added in later instars). Primary sensilla were coded by two capital letters, in most cases corresponding to the first two letters of the name of the structure on which they are located, and a number (setae) or a lower-case letter (pores). The following abbreviations were used: AB, abdominal segment VIII; AN, antenna; CO, coxa; FE, femur; FR, frontoclypeus; LA, labium; MN, mandible; MX, maxilla; PA, parietal; TA, tarsus; TI, tibia; TR, trochanter; UR, urogomphus. Setae

located at the apices of the antennae, maxillary and labial palpi were extremely difficult to distinguish due to their position and small size. Accordingly, they are identified as group (e.g., gAN = antennal group). The counting of secondary setae on selected structures of the *Rhantaticus* larva poses a difficulty knowing that first instar larvae of Aciliini possess a variable number of additional setae (Alarie *et al.* 2023a, 2023b). Faced with the absence of first instar larvae, putative additional setae present in *Rhantaticus* were therefore included in the number of secondary setae reported in this paper. Finally, a variable number of minute secondary setae are also found along the anterodorsal and posterodorsal margins of the coxae as well as on the posterior surface of femora and tibiae below the row of natatory setae. These setae are very difficult to count accurately because of their minute size and inconstant number. For this reason we have chosen to exclude them from our analysis and not to represent them in the figures concerned.

Phylogenetic analysis

To examine the phylogenetic signal of the larval characters of *Rhantaticus* and to test its relationships with other Aciliini, a cladistic analysis of five of the seven known genera of Aciliini (nine species) with sufficiently detailed larval descriptions (*Acilius*, *Graphoderus*, *Rhantaticus*, *Sandracottus*, *Thermonectus*) was conducted using the program TNT. The character database used in this study is largely similar to that used in a recent study of Aciliini larval morphology (Alarie *et al.* 2023b), although some characters are new or redefined. A total of 94 characters are incorporated into our study (Table 3; see the List at the end). *Notaticus fasciatus* Zimmermann, 1928 (tribe Aubehydrini), *Eretes australis* (Erichson, 1842) (tribe Eretini) and *Hydaticus tuyuensis* Trémouilles, 1996 (tribe Hydaticini), which are known to be related phylogenetically to the tribe Aciliini (Miller 2001, 2003; Michat & Alarie 2009; Alarie *et al.* 2011; Michat *et al*. 2017; Miller & Bergsten 2023), were used as out-groups. All characters were treated as equally weighted. Multistate characters were treated as non-additive. An exact solution algorithm (implicit enumeration) was implemented to find the most parsimonious trees. Bremer support values were calculated using the commands 'hold 20000', 'sub n' and 'bsupport', where 'n' is the number of extra steps allowed. The process was repeated increasing the length of the suboptimal cladograms by one step, until all Bremer values were obtained (Kitching *et al.* 1998). Bootstrap values were calculated using the following parameters: 'standard (sample with replacement)' and 1,000 replicates.

Results

General morphological characteristics of the larvae of *Rhantaticus* Sharp, 1882

Instar III larvae of *Rhantaticus* can readily be distinguished from those of other genera of Aciliini described in detail (i.e., *Acilius*, *Graphoderus*, *Sandracottus*, *Thermonectus*) by the following combination of characters: head capsule narrow, HL/HW > 1.70 (Figs 15–16); galea more than 2.00 times as long as maxillary palpomere 1 (Fig. 18); dorsal surface of stipes with two linear rows of spines (Fig. 18); maxillary palpomere 3 more than 1.70 times as long as maxillary palpomere 2 (Fig. 18); maxillary palpus less than 0.60 times length of labial palpus; median process of prementum unifid from base (cf. Figs 9–10); anterior surface of coxae lacking a row of hair-like setae (Fig. 19); proximal part of trochanter lacking elongate hair-like setae (Figs 19–20); terminal abdominal segment (LAS) less than 1.60 times length of HW; U/HW = 0.20.

Description of the instar II and III larvae of *Rhantaticus congestus* (Klug, 1833) (Figs 1–23)

Source of material. The larvae studied were associated with adults collected at the following localities: **Madagascar: Toliara:** RN10 15 km S. of junction RN7, Loc P44, muddy zebu waterhole, 23.24257S 44.22927E, 17.v.2006, one instar III (NHRS-JLKB000076336), leg. J. Bergsten. **Madagascar: Toliara: Menabe:** Kirindy RS. 20.07476S 44.67075E, 49 m.a.o. 12.xii.2009, MAD09-45, one instar II (NHRS-JLKB000000097, DNA voucher),

leg. J. Bergsten, N. Jönsson, T. Ranarilalatiana, J.H. Randriamihaja; **Madagascar: Toliara: Menabe:** Kirindy RS. 20.07655S 44.67532E, 65 m.a.o. 12.xii.2009, MAD09-47, one instar III (NHRS-JLKB000000098), leg. J. Bergsten, N. Jönsson, T. Ranarilalatiana, J. H. Randriamihaja; **Madagascar: Mahanjaga: Melaky:** btw Bekopaka – Antsalova. 18.91556S 44.55546E, 47 m.a.o. 16.xii.2009, MAD09-61, two instar II (NHRS-JLKB000075156), leg. J. Bergsten, N. Jönsson, T. Ranarilalatiana, J. H. Randriamihaja. **Madagascar: Fianarantsoa:** Plateau de l'Horombe, Nanarena vill. env; 22°30.1'S 45°45.6'E, 23.xi.2022, three instar II and nine instar III, leg. J. Hájek.

Description, instar II (Figs 1–14, 21–22)

Color: Body predominantly creamy white to pale yellow; head capsule yellow, with a median piceous macula on frontoclypeus and parietal; head appendages creamy white to pale yellow; thoracic terga and legs pale yellow; abdominal terga yellow except abdominal tergum VIII black over posterior half; urogomphi black. It is worth noting, however, that two deviating larvae, both collected from a residual pool in a dried-out forest stream in a closed canopy deciduous forest, were darker in colouration. This could reflect that pigmentation is adaptable in *R. congestus* being darker in forest habitats and lighter in open landscape ones.

Body: Subcylindrical, bent at first abdominal segment, gibbous in lateral view. Measurements and ratios aimed to characterize the body shape as in Table 1.

Head (Figs 1–10): Head capsule (Figs 1–2) flattened, subtriangular, longer than broad; maximum width at stemmata, not or slightly constricted at level of occipital region, HW/OCW = 2.29–2.39; occipital suture present, ecdysial line well marked; occipital foramen deeply emarginate both dorsally and ventrally; epicranial plates meeting ventrally, posterior tentorial pits visible ventrally on central region; surface smooth except for crescent-shaped microsculptures medially over occiput; frontoclypeus subtriangular, apical margin rounded medially; anterolateral lobes (= adnasalia) rounded, not projecting beyond nasale; six rounded dorsolateral stemmata at each side, stemmata protruding a short distance from head surface, two anterodorsal ones strongly developed. Antenna (Figs 3–4) short, robust, four-segmented, half as long as HW; A1 and A3 subequal in length, longest; A3 with a strongly developed ventroapical spinula; A4 shortest, with spinula at mid-length, similar to that of A3; apical lateroventral process of A3 (A3') not protruding; antennomeres not covered with short spine-like spinulae. Mandible (Figs 5–6) prominent, falciform, wide at base, sharp apically, with short-hair-like spinulae distally along inner margin; mandibular channel present, inner margin slightly toothed dorsally, more strongly ventrally. Maxilla (Figs 7–8) with cardo well developed; stipes strongly developed, subtrapezoidal, antero-internal angle right-angled, not projecting inwards, internal margin with short spinulae; palpifer very short, broad, incompletely sclerotized; palpus short, robust, three-segmented, MP1 shortest, MP3 longest, MP1/MP2 = 0.69–0.74; MP3 with spinula similar to those of antenna; palpomeres smooth, not covered with scattered minute spinulae; galea well developed, spiniform, slightly curved inwards, surface covered with scattered minute spinulae, GA/MP1 = 2.90–3.19. Labium (Figs 9–10) with prementum subtrapezoidal, somewhat pear-like, longer than broad, anterodorsal margin rounded, projecting forward into a unifid median process, not indented apically; dorsal surface of prementum densely covered with minute spine-like spinulae over apical and basal half; labial palpus short, robust, two-segmented, MP/LP = 0.66–0.69; palpomere 1 longest; palpomeres 1 and 2 with strong spine-like spinulae along external margin.

Thorax (Figs 11–12): Terga convex, pronotum about as long as meso- and metanotum combined, meso- and metanotum subequal; protergite subrectangular, margins truncated, more developed than meso- and metatergite; meso- and metatergite transverse, with anterotransverse carina; sagittal line well marked; venter membranous; spiracles absent. Legs (Figs 11–12): long, composed of six articles; L2 longest, slightly longer than subequal L1 and L3; CO robust, elongate, TR divided into two parts by an annulus, FE, TI and TA slender, subcylindrical, PT with two long, slender, almost straight claws, posterior claw shorter than anterior one; leg articles smooth, not covered with minute spine-like spinulae; ventral margin of protarsus with a row of well-developed spinulae along distal half; L3/HW = 2.89–3.05.

Abdomen (Figs 13–14): Eight-segmented, segments I–VI sclerotized dorsally, membranous ventrally; segments III–V widest, remaining segments progressively narrowing to apex; tergites I–VII similar to each other, narrow, transverse, laterally rounded, with anterotransverse carina, sagittal line present on anterior third; segments VII–VIII completely sclerotized; spiracles absent on segments I–VII; segment VIII (= LAS) (Fig. 13) longest, subtriangular, without anterotransverse carina, not covered with short spinulae; siphon reduced. Urogomphus (Fig. 14) short, one-segmented, not covered with short spinulae; U/HW = 0.38–0.45.

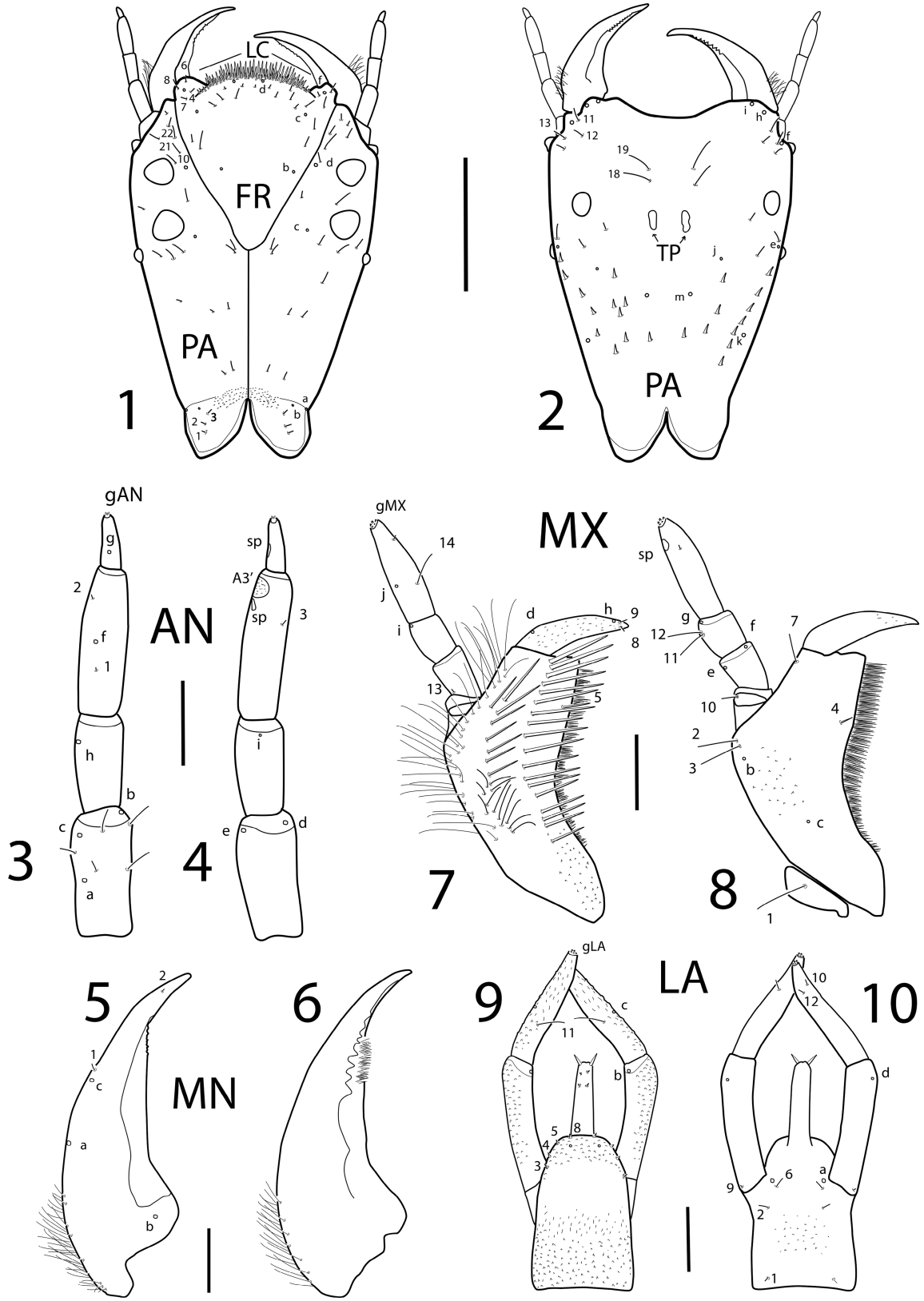

FIGURES 1–10. *Rhantaticus congestus* (Klug, 1833), instar II: 1. head capsule, dorsal aspect; 2. head capsule, ventral aspect; 3. antenna, dorsal aspect; 4. antenna, ventral aspect; 5. mandible, dorsal aspect; 6. mandible, ventral aspect; 7. maxilla, dorsal aspect; 8. maxilla, ventral aspect; 9. labium, dorsal aspect; 10. Labium, ventral aspect. AN, antenna, FR, frontoclypeus; gAN, antennal group; gMX, maxillary group; LA, labium; LC, lamellae clypeales; MN, mandible; MX, maxilla; PA, parietal; TP, tentorial pits; sp, spinula. Numbers and lowercase letters refer to primary setae and pores, respectively. Scale bars = 0.5 mm (Figs 1–2); 0.1 mm (Figs 3–10).

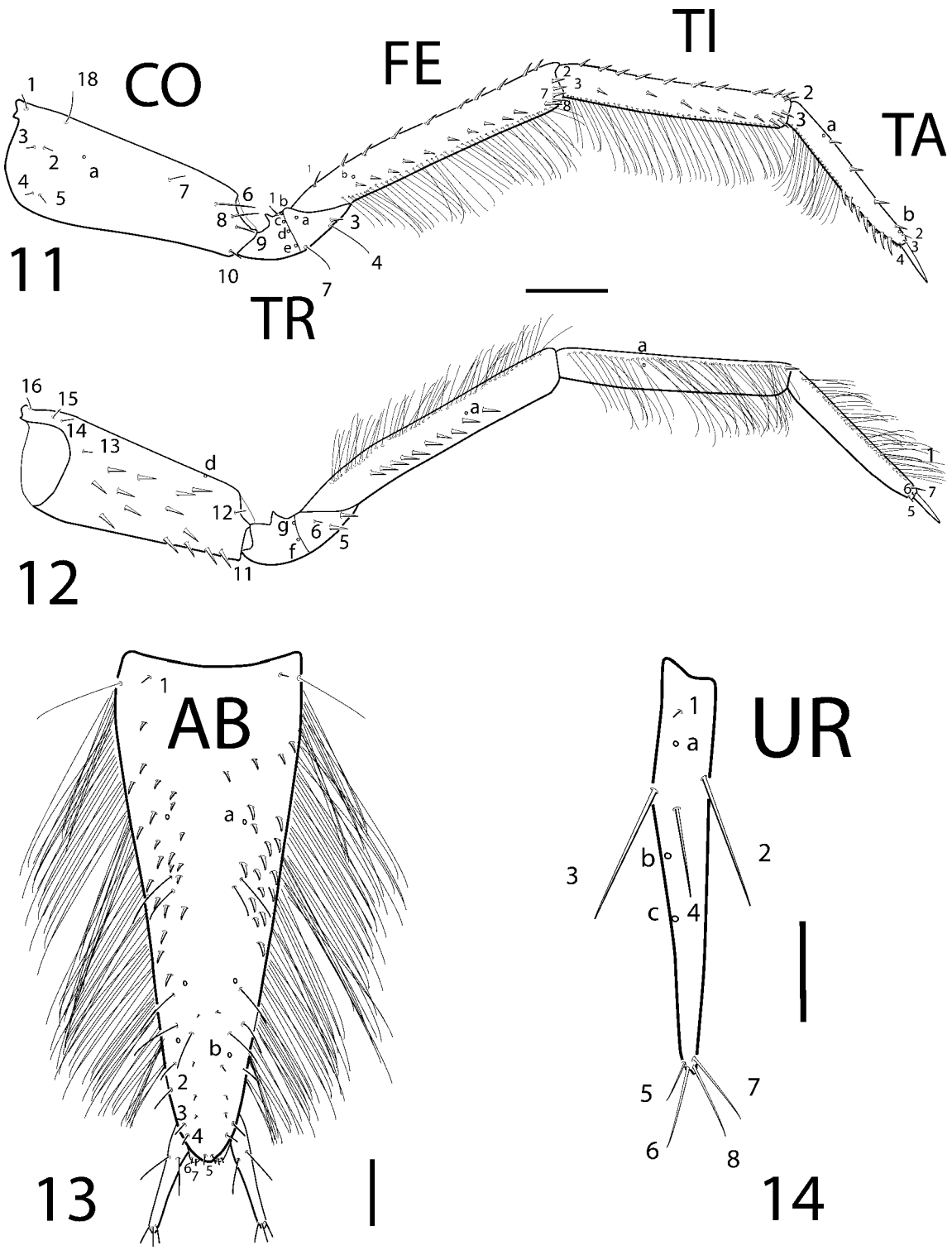

FIGURES 11–14. *Rhantaticus congestus* (Klug, 1833), instar II: 11. mesothoracic leg, anterior surface; 12. mesothoracic leg, posterior surface. 13. abdominal segment VIII, dorsal aspect; 14 urogomphus, dorsal aspect. AB, abdominal segment VIII; CO, coxa; FE, femur; TA, tarsus; TI, tibia; TR, trochanter; UR, urogomphus. Numbers and lowercase letters refer to primary setae and pores, respectively. Scale bars = 0.2 mm (Figs 11–13); 0.1 mm (Fig. 14).

Chaetotaxy (Figs 1–14): Dorsal surface of head capsule with few short secondary setae (Fig. 1); ventral surface of parietal with several spiniform setae (Fig. 2); antennomere I with several secondary setae dorsally (as in Fig. 17); mandible with a row of elongate secondary hair-like setae along basoexternal margin (Figs 5–6); dorsal surface of maxillary stipes with two rows of elongate spine-like setae, 20–21 along inner margin and 6–8 medially; numerous secondary hair-like setae present along the dorsoexternal margin of stipes (Fig. 7); secondary leg setation detailed in

Table 2; rows of secondary natatory setae present along posterodorsal margin and basal half of anteroventral margin of tarsi; posterior surface of femora and tibiae with linear row of minute secondary pores below the rows of natatory setae (not represented); abdominal segments VII–VIII with row of elongate natatory setae on lateral margin (Fig. 13); LAS with secondary spine-like setae dorsally and ventrally (Fig. 13).

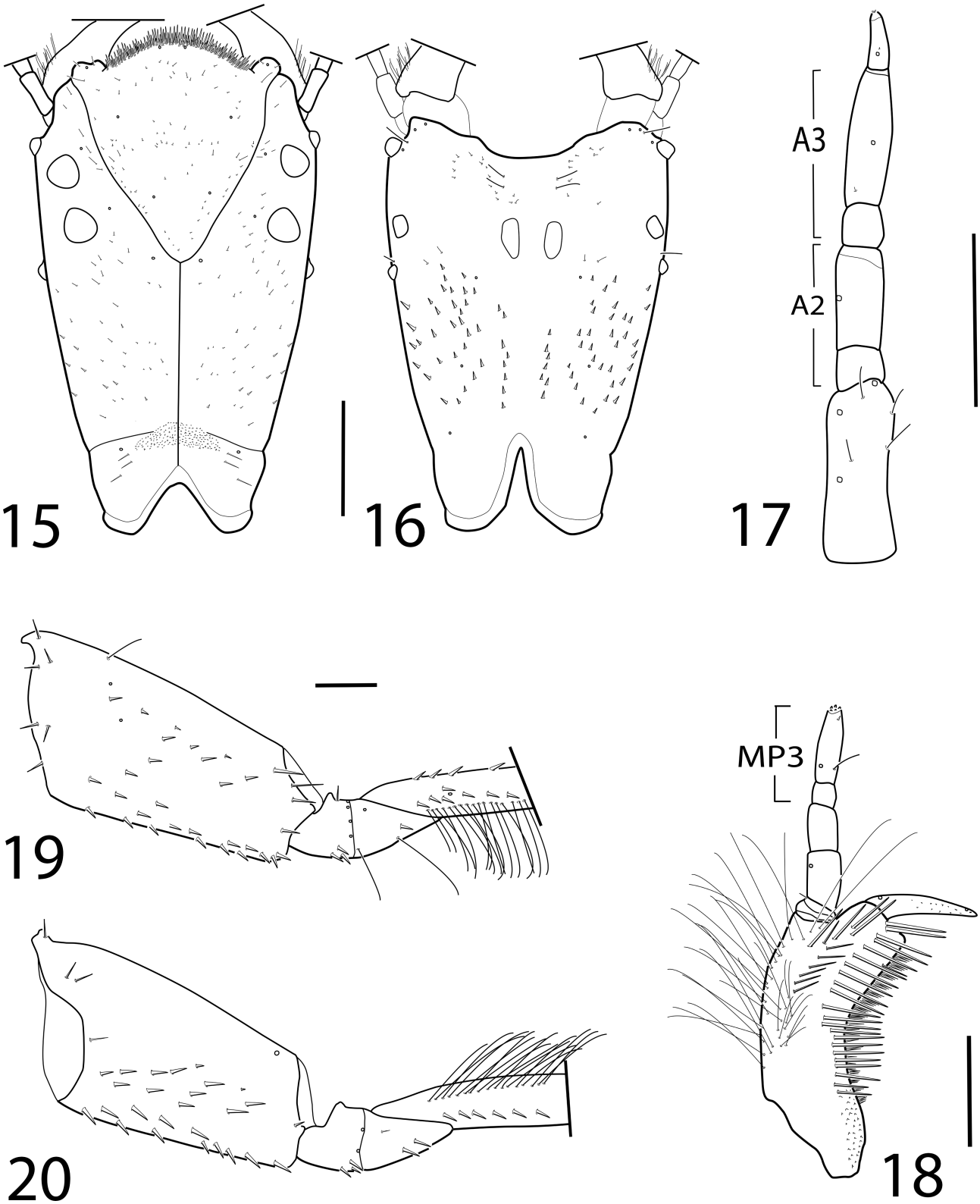

FIGURES 15-20. *Rhantaticus congestus* (Klug, 1833), instar III: 15. head, dorsal aspect; 16. head ventral aspect; 17. antenna, dorsal aspect; 18. maxilla, dorsal aspect; 19. mesocoxa and mesotrochanter, anterior surface; 20. mesocoxa and mesotrochanter, posterior surface. A, antennomere; MP, maxillary palpomere. Scale bars = 0.5 mm (Figs 15–16); 0.2 mm (Figs 17–20).

Description, instar III (Figs 15–20, 23)

As instar II except as follows:

Color: As in instar II (Fig. 23).

Body: Measurements and ratios aimed to characterise the body shape as in Table 1.

Head (Figs 15–18): Head capsule not constricted at level of occipital suture, HW/OCW = 1.83–1.97. Antenna: A2 and A3 secondarily subdivided (Fig.17). Maxilla: MP3 secondarily subdivided (Fig. 18); MP1/MP2 = 0.90–1.00; GA/MP1 = 2.36–2.54; MP/LP = 0.47–0.53.

Thorax (Figs 19–20): Spiracles present on mesothorax. Legs (Figs 19–20): L3/HW = 3.08–3.26.

Abdomen: Sagittal line and spiracles present on segments I–VII. Urogomphus: U/HW = 0.19–0.23.

Chaetotaxy (Figs 15–20): Parietal with several ventral secondary spine-like setae (Fig. 16); mandible with a larger number of minute secondary setae distally; dorsal surface of maxillary stipes 22–24 inner and 8–11 median spine-like setae (Fig. 18); secondary leg setation detailed in Table 2 and Figs 19–20.

Remarks: One instar II and two instar III larvae were CO1 sequenced along with two adults all collected in 2009. Latter two sequenced larvae were identical in 825bp of 3' end of COI with each other and with one adult female whereas an adult male from MAD09-47 had 3 differences.

Habitat and collecting circumstances: Except for the two larvae from Kirindy RS collected from a residual pool in a dried-out forest stream in a closed canopy deciduous forest, all specimens studied were sampled in open landscape temporary pools and ponds such as the one represented in Fig. 24 (size ca. 1.5 x 1.0 m; maximal depth about 0.5 m; muddy bed, surrounded with short Cyperaceae plants).

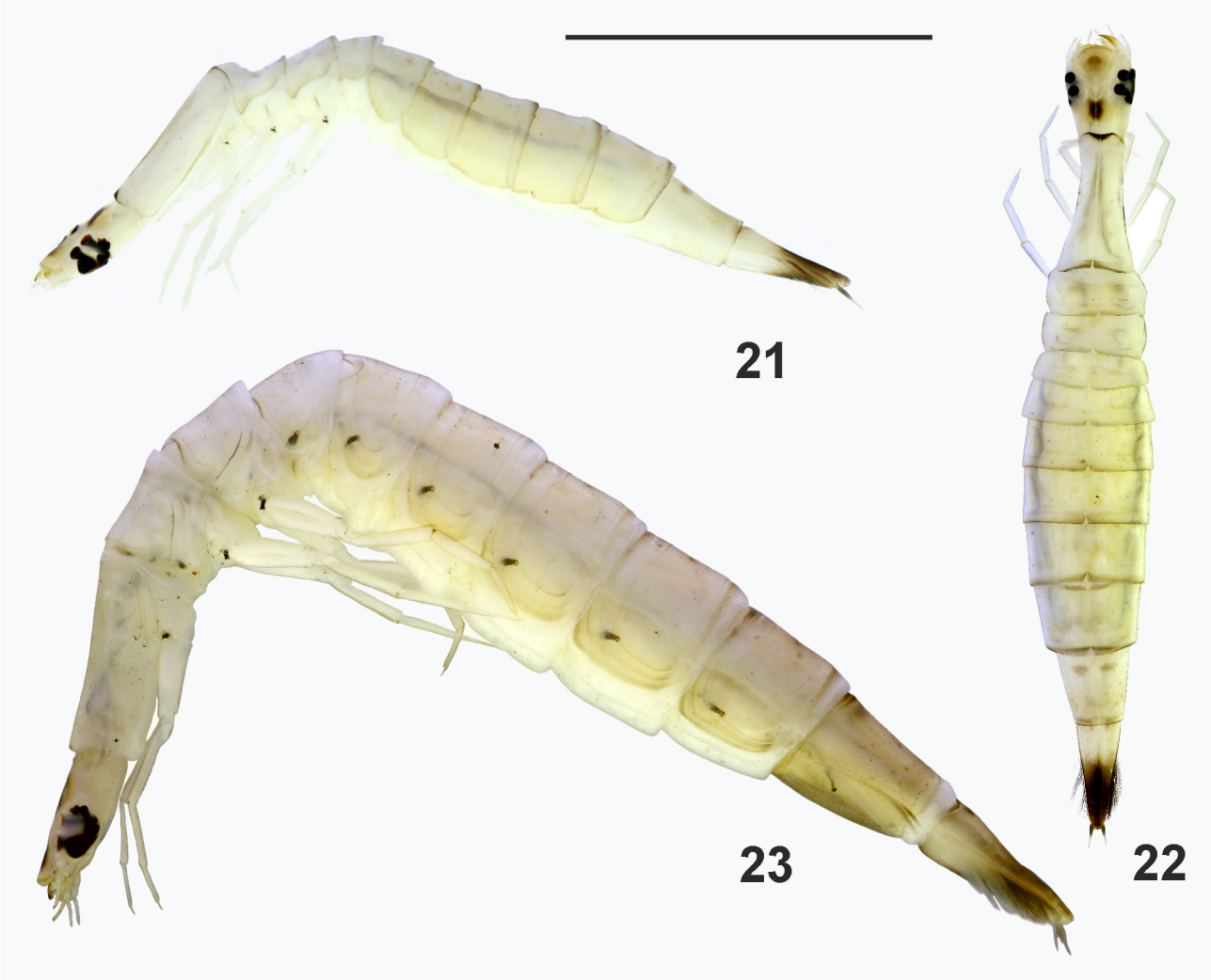

FIGURES 21-23. *Rhantaticus congestus* (Klug, 1833): 21. instar II, lateral aspect; 22. instar II, dorsal aspect; 23. instar III, lateral aspect. Scale bar = 5 mm.

Results of the parsimony analysis

The analysis of the data matrix with TNT resulted in seven most parsimonious trees of 125 steps (CI = 0.86; RI = 0.82). The strict consensus contained one polytomy (Fig. 25). Character state changes are mapped on one of the most parsimonious trees (Fig. 26). Whereas support for the monophyly of the Aciliini is very high (Bremer value = 6; bootstrap value = 99), the topology within this clade remains unresolved since only clades with congeneric taxa receive high Bootstrap values (Fig. 25).

FIGURE 24. Habitat of *Rhantaticus congestus* (Klug, 1833), temporary pool near Nanarena village, Plateau de l'Horombe.

Discussion

The description of *Rhantaticus congestus* larvae presented in this article brings to five the number of Aciliini genera whose larval morphology is known in detail (see Alarie *et al.* 2011, 2023b). Without great surprise, instar II–III larval morphology presents a series of characters which allow justifying the inclusion of the genus *Rhantaticus* among the Aciliini. Among these are the presence of a deeply emarginate occipital foramen dorsally (character 17; Figs 1, 15), the strongly developed ventroapical spinula on the antennomere 3 (character 28; Fig. 4), the presence of a row of secondary hair-like setae on the basolateral margin of the mandible (character 32; Figs 5–6), the secondary subdivision of the maxillary palpomere 3 (character 38; Fig. 18), and the lack of secondary subdivision of the maxillary palpomere 2 (character 40; Fig. 18).

When compared to other genera of Aciliini, larvae of *Rhantaticus* are distinguished by several unique character states: the narrower head capsule (character 02; Figs 1–2, 15–16) (HL/HW > 1.70 compared to < 1.50); the maxillary palpomere 3 relatively longer than the maxillary palpomere 2 (character 42) (more than 1.70 times compared to less than 1.60 times); the meso- and metacoxa of the third-stage larva lacking a line of hair-like setae on the anterior surface (character 68; Fig. 19); finally, the shorter instar III urogomphus relative to head width (character 93) (less than 0.20 times compared to more than 0.40 times).

Despite a larger number of species and genera as well as the addition of new characters (cf. Alarie *et al*. 2023b), our study failed at breaking a polytomy including all five aciliine genera studied (Fig. 25), each of which, however, emerging as morphologically distinct (Fig. 26). An underlying objective of this study was to compare the

Rhantaticus larva with that of *Sandracottus* given the suggested sister-group relationship between these two genera (Bukontaite *et al.* 2014). As previously demonstrated (Alarie *et al.* 2023b), the *Sandracottus* larva is distinguished among the Aciliini by the presence in the first-stage of more than 20 additional spiniform setae on the stipes as well as more than 23 additional natatory setae along the antero-ventral margin of the femur. In the absence of first instar larvae for *R. congestus*, however, we were not allowed to verify whether these conditions were also found in this species. Obviously, sampling more Aciliini species and genera would be needed to ascertain whether these characters are indeed synapomorphic for these two genera.

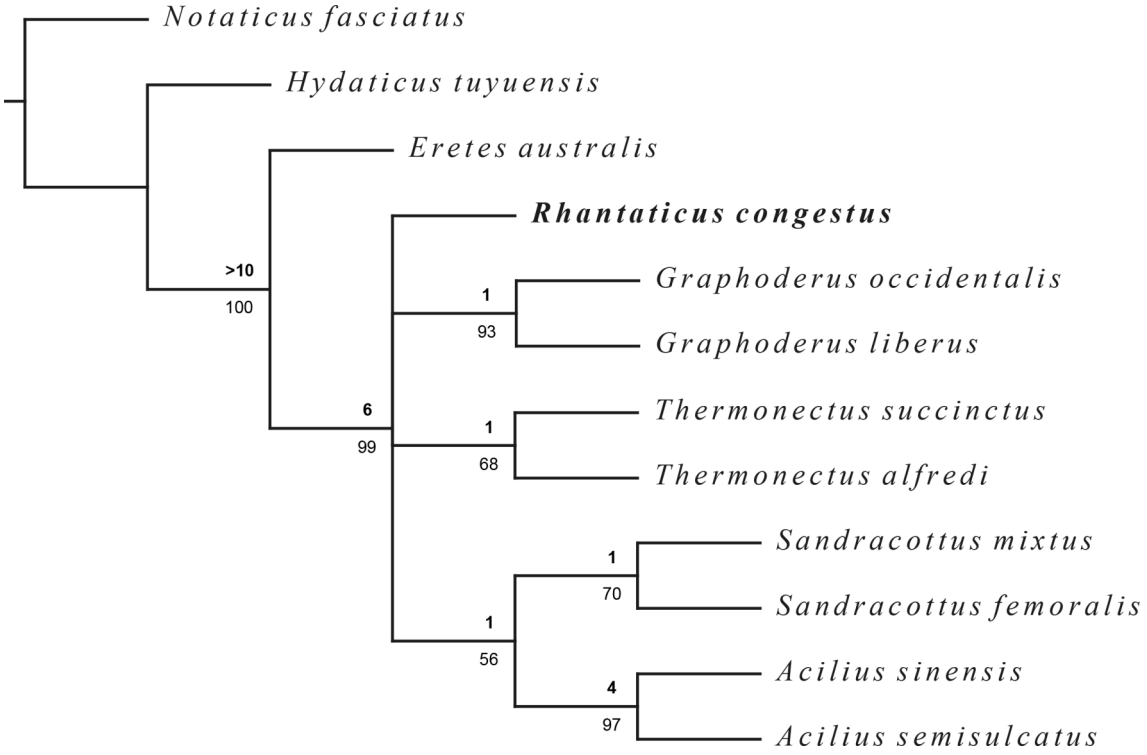

FIGURE 25. Strict consensus cladogram obtained from the cladistic analysis of 94 morphological characters scored for nine terminal taxa of Aciliini and three outgroups, with Bremer support values indicated above branches and Bootstrap support values higher than 50 indicated below branches.

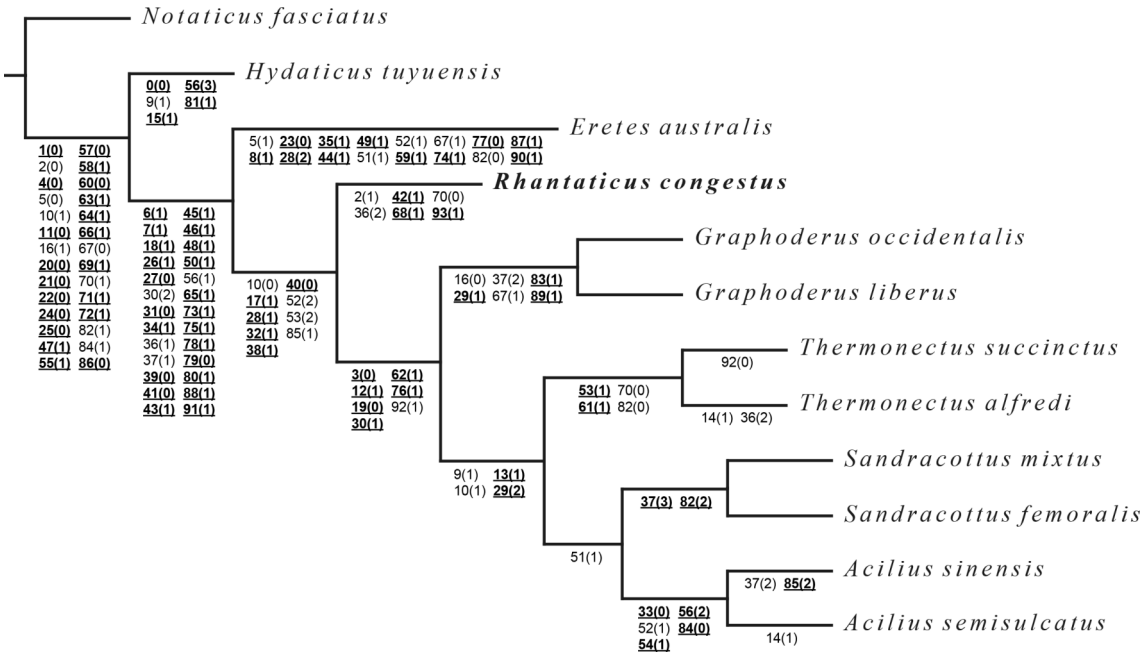

FIGURE 26. One of the most parsimonious trees obtained from the cladistic analysis, with character state changes mapped for each clade. Numbers in bold underlined indicate unique character state transformations.

TABLE 1. Measurements and ratios for larvae of *Rhantaticus congestus* (Klug, 1833).

Measure	Instar II (n = 4)	Instar III (n = 6)	Measure	Instar II (n = 4)	Instar III (n = 6)
HL (mm)	1.47–1.54	2.09–2.26	PMP/LP1	0.54–0.56	0.57–0.61
HW (mm)	0.91–0.93	1.20–1.30	MP/LP	0.66–0.70	0.47–0.53
FRL (mm)	0.69–0.74	0.95–1.05	LP2/LP1	0.66–0.81	0.63–0.71
OCW (mm)	0.39–0.41	0.61–0.68	L1 (mm)	2.67–2.87	3.59–3.86
HL/HW	1.59–1.65	1.67–1.80	L2 (mm)	2.78–2.99	3.85–4.17
HW/OCW	2.29–2.39	1.83–1.97	L3 (mm)	2.66–2.84	3.81–4.08
COL/HL	0.52–0.53	0.53–0.55	L3/L1	0.97–1.00	1.02–1.06
FRL/HL	0.47–0.48	0.45–0.47	L3/L2	0.95–0.96	0.97–0.99
A/HW	0.48–0.51	0.47–0.52	L3/HW	2.89–3.05	3.05–3.26
A1/A3	0.85–1.04	0.95–1.08	L3 (CO/FE)	0.93–0.95	1.02–1.10
A2/A3	0.67–0.78	0.83–0.95	L3 (TI/FE)	0.82–0.84	0.77–0.79
A4/A3	0.34–0.36	0.27–0.33	L3 (TA/FE)	0.63–0.65	0.56–0.59
MNL/MNW	2.69–2.89	2.76–2.90	L3 (CL/TA)	0.24–0.27	0.22–0.24
MNL/HL	0.33–0.34	0.32–0.35	LAS (mm)	1.43–1.58	1.95–2.05
PPF/MP1	0.46–0.58	0.37–0.43	LAS/HW	1.55–1.69	1.56–1.64
A/MP	1.78–1.84	1.64–1.77	U (mm)	0.35–0.42	0.40–0.47
MP1/MP2	0.69–0.79	0.90–1.00	U/LAS	0.24–0.26	0.33–0.34
MP3/MP2	1.91–2.20	1.73–2.14	U/HW	0.38–0.45	0.19–0.23
GA/MP1	2.90–3.19	2.36–2.54			

TABLE 2. Number and position of secondary setae on the legs of instar II and III of *Rhantaticus congestus* (Klug, 1833). Numbers between slash marks refer to pro-, meso- and metathoracic leg, respectively. A = anterior, AD = anterodorsal, AV = anteroventral, D= dorsal, Di = distal, NS = natatory setae, P = posterior, PD = posterodorsal, PV = posteroventral, Pr = proximal, sp = spiniform, V = ventral.

Segment	Position	Instar II (n = 4)	Instar III (n = 6)
Coxa	AD(NS)	0 / 0 / 0	0–1 / 0 / 0–1
	A(sp)	0–2 / 0–3/ 0	2–7 / 6–11 / 9–14
	P(sp)	2–8 / 4–9 / 1–3	6–11 / 10–16 / 7–15
	V(sp)	7–18 / 6–14 / 4–7	8–18 / 15–23 / 13–24
Trochanter	Pr(sp)	0–1 / 0–1 / 1	2–6 / 3–8 / 4–7
	Di(sp)	1 / 1 / 1–2	1–2 / 1–3 / 1
Femur	A(sp)	7–9 / 10–14 / 9–13	13–18 / 17–24 / 13–22
	AV (NS)	30–47 / 41–45 / 33–39	38–48 / 36–47 / 33–39
	D(sp)	7–9 / 9–10 / 10–12	14–22 / 19–26 / 18–22
	PDi(sp)	1 / 1 / 1	1–2 / 1 / 1
	V(sp)	7–19 / 10–16 / 0	15–17 / 13–18 / 8–11
	P(NS)	28–49 / 36–49 / 31–42	40–50 / 41–47 / 31–40
Tibia	A(sp)	0–1 / 8–10 / 9–10	3–8 / 10–14 / 13–16
	ADi(sp)	0 / 0 / 0	1–2 / 1–2 / 1–2
	AV(NS)	28–47 / 39–44 / 36–40	36–44 / 37–45 / 35–40
	D (sp)	5–9 / 10–11 / 16–18	10–13 / 11–17 / 17–26
	PDi(sp)	1 / 1–2 / 1	1–3 / 1–2 / 0–1
	PD(NS)	20–49 / 35–48 / 31–39	40–47 / 32–42 / 33–36
	PV(sp)	1–7 / 0–5 / 0	5–8 / 5–8 / 5–8
Tarsus	AD(sp)	3–5 / 2 / 2–4	4–5 / 2–5 / 5–7
	AV(sp)	7–9 / 5–7 / 6–8	7–10 / 4–8 / 4–7
	AV(NS)	17–19 / 19–21 / 20–24	17–18 / 16–19 / 17–24
	PD(NS)	29–37 / 29–34 / 28–34	29–34 / 32–35 / 30–33

Acknowledgments

The material from November 2022 was collected in the context of the DyticoBryo expedition led by M. Manuel (Sorbonne Université, Paris, France) and funded by the French "Agence Nationale de la Recherche" (grant ANR-19-CE02-003-01). Sampling was conducted under research permits No.82/06/MINENV.EF/SG/DGEF/DPB/SCBLF/RECH, No 266/09/MEF/SG/DGF/DCB.SAP/SLRSE, No 251/09/MEF/SG/DGF/DCB.SAP/SLRSE and N 336/22/MEDD/SG/DGGE/DAPRNE/SCBE.Re, and specimens were exported under permits No.167N-EA05/MG06, No 158N-EA12/MG09 and N°016N-EA01/MG23 issued by the "Ministère de l'Environnement et du Développement Durable" of the Republic of Madagascar. J. Hájek thanks all members of DyticoBryo expedition for wonderful three weeks together in Madagascar. This project was supported by Agencia Nacional de Promoción Científica y Tecnológica under Grant PICT–2017–1177 and by Universidad de Buenos Aires under Grant UBACyT–20020190100240BA (MCM). The work of JH was supported by the Ministry of Culture of the Czech Republic (DKRVO 2019-2023/5.I.e, National Museum, 00023272). J. Bergsten thanks all members of the 2006 and 2009 Madagascar expeditions and was supported by grants from the Swedish Research Council (Vetenskapsrådet, www.vr.se) (Grant numbers [#2009-3744] and [#2013-517]).

TABLE 3. Data matrix used for the cladistic analysis. Missing data coded '?'

Species	00	01	02	03	04	05	06	07	08	09	10	11	12	13	14	15	16	17	18	19	20	21	22	23	24	25	26	27	28	29	30	31	32	33	34	35	36	37	38	39	40	41	42	43	44	45	46
Notaticus fasciatus	1	1	1	1	1	1	0	0	0	0	0	1	0	0	0	0	0	0	0	1	1	1	1	1	1	1	0	1	0	0	0	1	0	1	0	0	0	0	0	1	1	1	0	0	0	0	0
Eretes australis	1	0	0	?	0	1	1	1	1	0	1	0	0	0	0	0	1	0	1	1	0	0	0	0	0	0	1	0	2	0	2	0	0	1	1	1	1	1	0	0	1	0	0	1	1	1	1
Hydaticus tuyuensis	0	0	0	1	0	0	0	0	0	1	1	0	0	0	0	1	1	0	0	1	0	0	0	1	0	0	0	1	0	0	0	1	0	1	0	0	0	0	0	1	1	1	0	0	0	0	0
Acilius semisulcatus	1	0	0	0	0	0	1	1	0	1	1	0	1	1	1	0	1	1	1	0	0	0	0	1	0	0	1	0	1	2	1	0	1	0	1	0	1	1	1	0	0	0	0	1	0	1	1
Acilius sinensis	1	0	0	0	0	0	1	1	0	1	1	0	1	1	0	0	1	1	1	0	0	0	0	1	0	0	1	0	1	2	1	0	1	0	1	0	1	2	1	0	0	0	0	1	0	1	1
Graphoderus liberus	1	0	0	0	0	0	1	1	0	0	0	0	1	0	0	0	0	1	1	0	0	0	0	1	0	0	1	0	1	1	1	0	1	1	1	0	1	2	1	0	0	0	0	1	0	1	1
Graphoderus occidentalis	1	0	0	0	0	0	1	1	0	0	0	0	1	0	0	0	0	1	1	0	0	0	0	1	0	0	1	0	1	1	1	0	1	1	1	0	1	2	1	0	0	0	0	1	0	1	1
Rhantaticus congestus	1	?	1	?	?	?	?	?	0	?	0	?	?	0	?	?	1	1	1	?	0	0	0	1	0	0	1	0	1	?	2	0	1	1	1	0	2	?	1	0	0	0	1	1	?	?	?
Sandracottus femoralis	1	0	0	0	0	0	?	?	0	1	1	0	1	1	0	0	1	1	1	0	0	0	0	1	0	0	1	0	1	2	1	0	1	1	1	0	1	3	1	0	0	0	0	1	0	1	1
Sandracottus mixtus	1	0	0	0	0	0	?	?	0	1	1	0	1	1	0	0	1	1	1	0	0	0	0	1	0	0	1	0	1	2	1	0	1	1	1	0	1	3	1	0	0	0	0	1	?	1	1
Thermonectus alfredi	1	0	0	0	0	0	1	1	0	1	1	0	1	1	1	0	1	1	1	0	0	0	0	1	0	0	1		1	2	1	0	1	1	1	0	2	1	1	0	0	0	0	1	0	1	1
Thermonectus succinctus	1	0	0	0	0	0	1	1	0	1	1	0	1	1	0	0	1	1	1	0	0	0	0	1	0	0	1	0	1	2	1	0	1	1	1	0	1	1	1	0	0	0	0	1	0	1	1

TABLE 3. Data matrix used for the cladistic analysis. Missing data coded '?' (continued)

Species	47	48	49	50	51	52	53	54	55	56	57	58	59	60	61	62	63	64	65	66	67	68	69	70	71	72	73	74	75	76	77	78	79	80	81	82	83	84	85	86	87	88	89	90	91	92	93
Notaticus fasciatus	0	0	0	0	0	0	0	0	0	0	1	0	0	1	0	0	0	0	0	0	1	0	0	0	0	0	0	0	0	0	1	0	1	0	0	0	0	2	0	1	0	0	0	0	0	0	0
Eretes australis	1	1	1	1	1	1	0	0	1	1	0	1	1	0	0	0	1	1	1	1	1	0	1	1	1	1	1	1	1	0	0	1	0	1	0	0	0	1	0	0	1	1	0	1	1	0	0
Hydaticus tuyuensis	1	0	0	0	0	0	0	0	1	3	0	1	0	0	0	0	1	1	0	1	0	0	1	1	1	1	0	0	0	0	1	0	1	0	1	1	0	1	0	0	0	0	0	0	0	0	0
Acilius semisulcatus	1	1	0	1	1	1	2	1	1	2	0	1	0	0	0	1	1	?	1	1	0	0	1	1	1	1	1	0	1	1	1	1	0	1	0	1	0	0	?	0	0	1	0	0	1	1	0
Acilius sinensis	1	1	0	1	1	1	2	1	1	2	0	1	0	0	0	?	1	1	1	1	0	0	1	1	1	1	1	0	1	1	1	1	0	1	0	1	0	0	2	0	0	1	0	0	1	1	0
Graphoderus liberus	1	1	0	1	0	2	2	0	1	1	0	1	0	0	0	1	1	1	1	1	1	0	1	1	1	1	1	0	1	1	1	1	0	1	0	1	1	1	1	0	0	1	1	0	1	?	?
Graphoderus occidentalis	1	1	0	1	0	2	2	0	1	1	0	1	0	0	0	1	1	1	1	1	1	0	1	?	1	1	1	0	1	1	1	1	0	1	0	1	1	1	?	0	0	1	1	0	1	1	?
Rhantaticus congestus	1	1	0	?	?	2	2	?	1	1	0	1	0	0	0	?	?	1	1	1	0	1	1	0	?	?	?	0	1	?	1	1	0	1	0	?	?	?	1	0	0	?	?	?	1	?	1
Sandracottus femoralis	1	1	0	1	1	2	2	0	1	1	0	1	0	0	0	?	1	1	1	1	0	0	1	1	1	1	1	0	1	1	1	1	0	1	0	2	0	1	1	0	0	1	0	0	1	1	0
Sandracottus mixtus	1	1	0	1	1	2	2	0	1	1	0	1	0	0	0	?	1	1	1	1	0	0	1	1	1	1	1	0	1	1	1	1	0	1	0	2	0	1	1	0	0	1	0	0	1	1	0
Thermonectus alfredi	1	1	0	1	0	2	1	0	1	1	0	1	0	0	1	1	1	1	1	1	0	0	1	0	1	1	1	0	1	1	1	1	0	1	0	0	0	1	1	0	0	1	0	0	1	?	0
Thermonectus succinctus	1	1	0	1	0	2	1	0	1	1	0	1	0	0	1	1	1	1	1	1	0	0	1	0	1	1	1	0	1	1	1	1	0	1	0	0	0	1	1	0	0	1	0	0	1	0	0

List: Characters used for the phylogenetic analysis and the coding of states using the genera *Eretes* Laporte, 1833 (Eretini), *Notaticus* Zimmermann, 1928 (Aubehydrini), and *Hydaticus* Leach, 1817 (Hydaticini) as outgroups.

00. Body (instars 1–III): (0) not gibbous in lateral view; (1) gibbous in lateral view.
01. Multi-branched setae on the body (instar I): (0) absent; (1) present.
02. Head capsule (instar III): (0) broader, HL/HW < 1.50; (1) narrower, HL/HW > 1.70.
03. Primary seta FR9 (instar I): (0) inserted close to seta FR10; (1) inserted far from seta FR10.
04. Egg bursters (instar I): (0) located submedially on the frontoclypeus, close to frontal suture; (1) located proximally on the frontoclypeus.
05. Primary pore FRf (instar I): (0) present; (1) absent.
06. Setae FR3, PA16, PA19 and AB9 (instar I): (0) not lanceolate; (1) lanceolate.
07. Setae FR9 and FR10 (instar I): (0) visible in dorsal view, inserted laterally to lamellae clypeales; (1) not visible in dorsal view, inserted ventrally to lamellae clypeales.
08. Lamellae clypeales (instars I–III): (0) digitiform to spatulate; (1) bifid.
09. Parietals (at level of occipital suture) (instar I): (0) not constricted; (1) constricted.
10. Parietals (at level of occipital suture) (instars II–III): (0) not constricted; (1) constricted.
11. Primary pore PAa (instar I): (0) dorsal; (1) ventral.
12. Primary pore PAl (instar I): (0) present; (1) absent.
13. Primary pore PAm (instar I): (0) present; (1) absent.
14. Primary pore PAo (instar I): (0) present; (1) absent.
15. Occipital suture (instar I): (0) absent; (1) present.
16. Occipital suture (instars II–III): (0) absent; (1) present.
17. Occipital foramen (instars I–III): (0) not or slightly emarginate dorsally; (1) deeply emarginate dorsally.
18. Stemmata (instars I–III): (0) subequal in size; (1) anterodorsal two strongly developed.
19. Ventral surface of parietal (instar 1): (0) lacking additional setae; (1) with one VAp marginal additional seta.
20. Multifid setae on cephalic capsule and abdominal segment VIII (instars I–III): (0) absent; (1) present.
21. Primary seta AN1 (instar I): (0) proximal to median; (1) distal.
22. Primary seta AN3 (instar I): (0) articulated sub-distally; (1) articulated apically.
23. Primary pore ANc (instar I): (0) at about same level of pore ANb; (1) somewhat more proximal than pore ANb.
24. Primary pore ANf (instar I): (0) median to proximal; (1) subdistal.
25. Primary pore ANg (instar I): (0) located basally; (1) located medially.
26. Primary pore ANi (instar I): (0) sub-median; (1) sub-distal to sub-apical.
27. Antennomeres 2 and 3 (instar II): (0) not subdivided; (1) subdivided in two articles.
28. Ventroapical spinula on antennomere 3 (instars I–III): (0) minute; (1) strongly developed; (2) absent.
29. Antennomeres 1 and 2 (instar I): (0) lacking spinulae; (1) with spinulae along apical margin; (2) with spinulae over most surface.
30. Apical lateroventral process of antennomere 3 (instars I–III): (0) protruding (digitiform);(1) protruding (rounded or dentate); (2) not protruding.
31. Primary seta MN1 (instar I): (0) inserted more distally than pore MNc; (1) inserted more proximally than pore MNc.
32. Row of secondary hair-like setae on laterobasal margin of mandible (instars II–III): (0) absent; (1) present.
33. Primary pore MNa (instar I): (0) inserted at approximately the same level as pore MNb; (1) inserted distally to pore MNb.
34. Stipes (instar I): (0) narrow, subcylindrical; (1) robust, subtrapezoidal to subtriangular.
35. Anterior mesal margin of stipes (instars I–III): (0) without lacinia, spines or robust spinulae; (1) with a spiniform lacinia projected inward.
36. Stipes (instar II–III): (0) lacking dorsal row of spine-like setae; (1) with one row of spine-like setae; (2) with two rows of spine-like setae.
37. Dorsolateral row of additional spine-like setae on dorsal surface of stipes (instar I): (0) absent; (1) less than 12; (2) 13–19; (3) > 20.

38. Palpifer (instars I–III): (0) similar to a palpomere, clearly differentiated from stipes dorsally; (1) inconspicuous, not clearly differentiated from stipes dorsally.
39. Maxillary palpomere 2 (instar II): (0) not subdivided; (1) subdivided into two articles.
40. Maxillary palpomere 2 (instar III): (0) not subdivided; (1) subdivided into two articles.
41. Maxillary palpomere 3 (instar II): (0) not subdivided; (1) subdivided into two articles.
42. Ratio maxillary palpomere 3/maxillary palpomere 2 (instar III): (0) <1.60; (1) > 1.70.
43. Lateroventral subapical process of maxillary palpomere 3 (instars I–III): (0) absent; (1) present.
44. Primary setae MX2, MX3 and LA11 (instar I): (0) not lanceolate; (1) lanceolate.
45. Seta MX6 (instar I): (0) present; (1) absent.
46. Seta MX14 (instar I): (0) inserted submedially; (1) inserted at basal third or more basally.
47. Additional setae on maxillary palpomere 3 (instar I): (0) absent; (1) present.
48. Row of long hair-like secondary setae along external margin of stipes (instar II–III): (0) absent; (1) present.
49. Secondary setae on maxillary palpomere 1 (instars II–III): (0) absent; (1) present.
50. Spinulae on stipes (instar I): (0) absent; (1) present.
51. Spinulae on galea (instar I): (0) present; (1) absent.
52. Galea (instar III): (0) shorter than maxillary palpomere 1; (1) longer than maxillary palpomere 1, GA/MP1 < 1.50; (2) much longer than maxillary palpomere 1, GA/MP1 > 2.00.
53. Maxillary palpus (instar III): (0) > 1.30 times length of labial palpus, ; (1) 0.70–1.10 times length of labial palpus; (2) < 0.60 times length of labial palpus.
54. Maxillary palpomeres (instar I): (0) spinulae lacking; if present reduced to apical margin of palpomeres 1 and 2; (1) with abundant spinulae on every palpomere.
55. Anterior margin of prementum (instar I): (0) straight to slightly emarginate; (1) projected forward.
56. Median process of prementum (instars I–III): (0) absent; (1) unifid; (2) bifid beyond the base; (3) bifid from the base, as two separate lobes.
57. Primary seta LA6 (instar I): (0) inserted distally; (1) inserted submedially.
58. Primary seta LA8 (instar I): (0) absent; (1) present.
59. Primary seta LA10 (instar I): (0) inserted distally; (1) inserted submedially.
60. Primary pore LAc (instar I): (0) inserted submedially; (1) inserted proximally.
61. Additional setae on dorsal surface of prementum (instar I): (0) absent; (1) present.
62. Additional pore on dorsal surface of prementum (instar I): (0) absent; (1) present.
63. Additional setae on labial palpomere 2 (instar I): (0) absent; (1) present.
64. Secondary setae on prementum (instars II–III): (0) absent; (1) present.
65. Dorsal surface of prementum (instar I): (0) lacking spinulae; (1) densely covered with spinulae.
66. Lateral margin of labial palpomeres 1 and 2 (instar I): (0) lacking spinulae; (1) densely covered with spinulae.
67. Primary seta CO7 on meso- and metacoxa (instar I): (0) inserted submedially to distally; (1) inserted proximally.
68. Meso- and metacoxa (instar III): (0) with a row of anterior hair-like setae; (1) lacking anterior hair-like setae.
69. Primary seta TR2 (instar I): (0) present; (1) absent.
70. Metatrochanter (instar III): (0) lacking proximal hair-like secondary setae; (1) with a variable number of proximal secondary hair-like setae.
71. Primary seta TI1 (instar I): (0) inserted submedially to distally; (1) inserted apically.
72. Primary seta TI5 (instar I): (0) short, spine-like; (1) elongate, hair-like.
73. Primary seta TI5 on metatibia (instar I): (0) inserted distally; (1) inserted more proximally.
74. Primary seta TA5 (instar I): (0) inserted posteroventrodistally; (1) inserted posterodorsodistally.
75. Primary pore TAa (instar I): (0) inserted submedially to distally; (1) inserted proximally.
76. Primary pores TAc, TAd, TAe and TAf (instar I): (0) present; (1) absent.
77. Secondary dorsal setae on protarsus (instars II–III): (0) absent; (1) present.
78. Natatory anteroventral setae on tarsus (instars II–III): (0) absent; (1) present.
79. Basoventral patch of dense slender spinulae on protarsus (instars II–III): (0) absent; (1) present.
80. Primary setae PT1 and PT2 (instar I): (0) present; (1) absent.
81. Basoventral spinulae on claws (instars I–III): (0) absent; (1) present.
82. AV additional natatory setae on femur (instar I): (0) less than 12; (1) 13–23; (2) > 23.

83. Abdominal tergites I–VI (instar I): (0) with anterotransverse carina; (1) without anterotransverse carina.
84. Abdominal segment VII (instar I): (0) sclerotized dorsally, membranous ventrally; (1) completely sclerotized except for a narrow longitudinal ventral band; (2) completely sclerotized, ring-like.
85. Abdominal segment VIII (LAS) (instar III): (0) shorter or about as long as HW; (1) 1.20–1.60 times HW; (2) > 1.80 times HW.
86. Primary seta AB6 (instar I): (0) present; (1) absent.
87. Primary seta AB13 (instar I): (0) present; (1) absent.
88. Primary pore ABc (instar I): (0) present; (1) absent.
89. Additional pores on dorsal surface of abdominal segment VIII (instar I): (0) absent; (1) present.
90. Natatory setae on lateral margin of abdominal segment VII (instar I): (0) absent; (1) present.
91. Primary seta UR5 (instar I): (0) long, hair-like; (1) short, spine-like.
92. Primary seta UR7 (instar I): (0) shorter than setae UR6 and UR8; (1) as long as setae UR6 and UR8;
93. Urogomphus (instar III): (0) > 0.40 times as long as HW; (1) < 0.20 times as long as HW.

References

Alarie, Y., Mai, Z., Michat, M.C. & Hájek, J. (2023a) Larval morphology and new records of the iconic diving beetle *Acilius sinensis* Peschet, 1915 (Coleoptera: Dytiscidae: Dytiscinae) – a species well established in western Yunnan, China. *Zootaxa*, 5301 (2), 277–291.
https://doi.org/10.11646/zootaxa.5301.2.8

Alarie, Y. & Michat. M.C. (2023) Larval chaetotaxy of world Dytiscidae (Coleoptera: Adephaga) and implications for the study of Hydradephaga. *In*: Yee, D.A. (Ed.), *Ecology, systematics, and the natural history of predaceous diving beetles (Coleoptera: Dytiscidae)*. *Second Edition*. Cham: Springer Nature Switzerland AG, pp. 17–53.
https://doi.org/10.1007/978-3-031-01245-7_2

Alarie, Y., Michat, M.C. & Miller, K.B. (2011) Notation of primary setae and pores on larvae of Dytiscinae (Coleoptera: Dytiscidae), with phylogenetic considerations. *Zootaxa*, 3087 (1), 1–55.
https://doi.org/10.11646/zootaxa.3087.1.1

Alarie, Y., Michat, M.C., Shaverdo, H. & Hájek, J. (2023b) Morphology of the larvae of *Sandracottus femoralis* Heller, 1934, and *S. mixtus* (Blanchard, 1843) and phylogenetic comparison with other known Aciliini (Coleoptera: Dytiscidae, Dytiscinae). *Zootaxa*, 5263 (3), 301–334.
https://doi.org/10.11646/zootaxa.5263.3.1

Bertrand, H. (1972) *Larves et nymphes des coléoptères aquatiques du Globe*, Paris: Imprimerie F. Paillart, 804 pp.

Bukontaite, R., Miller, K.B. & Bergsten, J. (2014) The utility of CAD in recovering Gondwanan vicariance events and the evolutionary history of Aciliini (Coleoptera: Dytiscidae). *BMC Evolutionary Biology*, 14, 5 (18 pp.).
https://doi.org/10.1186/1471-2148-14-5

Dejean, P.F.M.A. (1833) *Catalogue des coléoptères de la collection de M. le Comte Dejean*, Paris, 176 pp.
https://doi.org/10.5962/bhl.title.8771

Erichson, G.W.F. (1842) Beitrag zur Insecten-fauna von Vamdiemensland mit besonderer Berücksichtigung der geographischen Verbreitung der Insecten. *Archiv für Naturgeschichte*, 8, 83–287.
https://doi.org/10.5962/bhl.part.21657

Kitching, I.J., Forey, P.L., Humphries, C.J. & Williams, D.M. (1998) *Cladistics, Second Edition. The theory and practice of parsimony analysis*. Systematic Association publications, 11. New York, Oxford University Press, 228 pp.

Klug, J.C.F. (1833) *Bericht über eine auf Madagascar veranstaltete Sammlung von Insecten aus der Ordnung Coleoptera*. Berlin: Königlichen Akademie der Wissenschaften, 135 pp. + 5 pls.

Leach, W.E. (1817) XIX. Synopsis of the stirpes and genera of the family Dyticidea, pp. 68–73. *In*: *The zoological miscellany; being descriptions of new or interesting animals*. Vol. 3. London: E. Nodder & Son, v + 151 pp. + pls 121–150.

Michat, M.C. (2013) Description of the larvae of *Thermonectus alfredi* Griffini, 1898 (Coleoptera: Dytiscidae). *Koleopterologische Rundschau*, 83, 7–15.

Michat, M.C. & Alarie, Y. (2009) Phylogenetic relationships of *Notaticus* (Coleoptera: Dytiscidae) based on larval morphology. *Annals of the Entomological Society of America*, 102, 797–808.
https://doi.org/10.1603/008.102.0506

Michat, M.C., Alarie, Y. & Miller, K.B. (2017) Higher-level phylogeny of diving beetles (Coleoptera: Dytiscidae) based on larval characters. *Systematic Entomology*, 42, 734–767.
https: //doi.org/ 10.1111/syen.12243

Michat, M.C. & Torres, P.L.M. (2005) Larval morphology of *Thermonectus succinctus* (Aubé 1838) (Coleoptera: Dytiscidae: Dytiscinae), with biological notes and chaetotaxic analysis, *Aquatic Insects*, 27, 281–292.
https://doi.org/10.1080/01650420500294021

Michat, M.C. & Torres, P.L.M. (2016) *Thermonectus tremouillesi* sp. nov. (Coleoptera: Dytiscidae: Aciliini): description of the

adults and larvae and comparisons with other species of the genus. *Journal of Natural History*, 50, 1633–1648. https://doi.org/10.1080/00222933.2016.1145274
Miller, K.B. (2001) On the phylogeny of the Dytiscidae (Coleoptera) with emphasis on the morphology of the female reproductive system. *Insect Systematics and Evolution*, 32, 45–92. https://doi.org/10.1163/187631201X00029
Miller, K.B. (2003) The phylogeny of diving beetles (Coleoptera: Dytiscidae) and the evolution of sexual conflict. *Biological Journal of the Linnaean Society*, 79, 359–388. https://doi.org/10.1046/j.1095-8312.2003.00195.x
Miller, K.B., Alarie, Y. & Whiting, M.F. (2007) Description of the larva of *Notaticus fasciatus* (Coleoptera: Dytiscidae) associated with adults using DNA sequence data. *Annals of the Entomological Society of America*, 100, 787–797. https://doi.org/10.1603/0013-8746(2007)100[787:DOTLON]2.0.CO;2
Miller, K.B. & Bergsten, J. (2016) *Diving beetles of the world. Systematics and biology of the Dytiscidae*. Baltimore: Johns Hopkins University Press, 320 pp. https://doi.org/10.1093/ae/tmx033
Miller, K.B. & Bergsten, J. (2023) The phylogeny and classification of predaceous diving beetles (Coleoptera: Dytiscidae). *In*: Yee, D.A (Ed.), *Ecology, systematics, and the natural history of predaceous diving beetles (Coleoptera: Dytiscidae)*. *Second Edition*. Cham: Springer Nature Switzerland AG, pp. 55–185. https://doi.org/10.1007/978-3-031-01245-7_3
Nilsson, A.N. (1988) A review of primary setae and pores on legs of larval Dytiscidae (Coleoptera). *Canadian Journal of Zoology*, 66, 2283–2294. https://doi.org/10.1139/z88-339
Nilsson, A.N. & Hájek, J. (2023) *A world catalogue of the family Dytiscidae, or the diving beetles (Coleoptera, Adephaga). Version 1.I.2023*. Distributed as a PDF file via Internet. Available from: http://www.waterbeetles.eu (accessed 03 May 2023)
Omer-Cooper, J. (1956) *Tikoloshanes*, a new genus of Dytiscidae (Col.) from South Africa. *Proceedings of the Royal Entomological Society of London (B)*, 25, 79–82. https://doi.org/10.1111/j.1365-3113.1956.tb01095.x
Sharp, D. (1882) On aquatic carnivorous Coleoptera or Dytiscidae. *The Scientific Transactions of the Royal Dublin Society, Series 2*, 2, 179–1003 + pls. 7–18. https://doi.org/10.5962/bhl.title.9530
Trémouilles, E.R. (1996) Revisión del género *Hydaticus* Leach en América del sur, con descripción de tres nuevas especies. *Physis, Buenos Aires*, 52B (122–123) (1994), 15–32.
Wiley, E.O. (1981) *Phylogenetics. The theory and practice of phylogenetic systematics*. John Wiley and Sons, New York, USA, 439 pp.
Zimmermann, A. (1928) Neuer Beitrag zur Kenntnis der Schwimmkäfer. *Wiener Entomologische Zeitung*, 44, 165–187.